www.gondwanags.org.in

Research Article

ISSN : 2455-1953

JGSR

Journal of Geosciences Research

Vol. 10, No.1, January, 2025, pp. 30-35

Elemental Mobility and Crustal Contamination of Metabasalts Around Bisnal Area, Karnataka, India with Emphasis on Trace Element Geochemistry

Thanmaya B.M. [1]*, Mahantesha. P.[2], Prakash Narasimha K.N.[1] and Suresh Kumar B.V.[1]

[1]*Department of Studies in Earth Science, University of Mysore, Manasagangotri, Mysore-570006 (KN), India*

[2]*Indian Bureau of Mines, Yeshwanthpur, Bengaluru-560022 (KN), India*

*(*Corresponding Author, E-mail: bandikanethanmaya@gmail.com)*

Abstract

The present work includes the study of the metabasalt samples collected from Bisnal village of Bagalkot District, Karnataka which forms the northwest extension of the Hungund Kushtagi (H-K) schist belt, belonging to the Eastern Dharwar Craton (EDC), indicates upper greenschist to epidote amphibolite facies of metamorphism. These rocks have also undergone the process of hydrothermal alteration, which is evidenced by the occurrence of pyrite and chalcopyrite in the quartzcarbonate veins. These metabasalts show compositional variation from basalts to andesite which is determined by the ratios of Nb/Y *vs* Zr/Ti and Nb/Y *vs* Zr/TiO_2. The slight enrichment of the LILE and LREE elements with the LREE/HREE ratio (1.70-2.17), the HREE ratio (1.09-1.13) and the negative Eu/Eu* ratio for all samples with a range of 0.89-0.93 indicates that these rocks have undergone low to moderate fractionation process during crystallization. Elements such as Na, K, Ca and the HFSE elements such as Nb, Th, Zr, Hf, and Ta show slight deviation from their normal values, and the variation in the Ce/Ce* ratios, indicates the elemental mobility and the magma crust interaction process. The Lower values of Ni, Cr and higher ratios of Th/La, than that of the primitive mantle and the Nb/Y ratios to that of the lower crust indicates that these metabasalts have undergone the crustal contamination processes.

Keywords: Metabasalt, Amphibolite, Trace Elements, REE, Geochemistry

Introduction

The metabasalts in the vicinity of Bisnal village, located in the NW region of Bagalkot district, are part of the unique Hungund-Kushtagi (H-K) schist belts (Dey *et al.*, 2012) The metabasalts, with an age of 3.0 Ga, which are part of EDC, are of significant interest as it hosts various economic mineral deposits such as gold, copper and cobalt (Mahantesha *et al.*, 2021). They provide a window into the region's geological past, particularly the Archean era (Naqvi *et al.*, 2006; Manikyamba *et al.*, 2021).The Archean crust, where these rocks are found, is a crucial key to understanding the cores of proto continents (Singh *et al.*, 2020).

The metabasaltic rocks play a pivotal role in providing detailed insights into processes such as mantle melting and P-T conditions during the crustal melting (Patra et al., 2020) and various tectonic processes(Manikyamba *et al.*, 2014; Condie and Kröner, 2013; Condie and Aster, 2013) . Understanding the degree of melting and the type of interaction between the crust and mantle is crucial in determining the source of these rocks (Patra *et al.*, 2020). Rocks of the archean age also provide insight into the several metamorphic, magmatic and mineralization processes that have happened over geological time (Manikyamba *et al.*, 2014; Pearce, 2014; Weaver and Tarney, 1981) .

The komatiites and the basaltic rocks of 2.5 Ga show the decrease in incompatible elements at the upper mantle, which is evidenced by the higher ratios of the Nb/Th and Nb/U ratios (Manikyamba *et al.*, 2015; Singh *et al.*, 2020). This is also the reason for the extraction of the mantle melt from the mafic and ultramafic rocks, which has led to the formation of continental crust (Singh *et al.*, 2020; Taylor and McLennan, 1995; Polat, 2012; Kerrich and Xie, 2002; Bennett, 2003; Manikyamba *et al.*, 2015).

During the formation of the Archean crust, several processes operated, such as subduction zone phenomena such as plume arc magmatism, flat slab oceanic subduction, and oceanic ridge subduction(Singh *et al.*, 2020), which indicates a hot mantle condition (Manikyamba *et al.*, 2015, 2021; Pearce, 2014). The geological setting of the EDC suggests that they have formed under interaoceanic and mantle plume accretionary conditions (Manikyamba *et al.*, 2014). The greenstone rocks of the EDC show the plume magmatism and plume continental interaction, which is evident in the rocks of komatiite and basalts. In contrast, the subduction accretion process can be seen in the “tholeiitic to calc-alkaline basalt, andesite, dacite, and rhyolite (BADR) rocks” (Manikyamba *et al.*, 2015, 2021). Moreover, the active tectonic process is seen at EDC (Manikyamba *et al.*, 2021; Pahari *et al.*, 2019; Singh *et al.*, 2020). The present study discusses the

(Received : 04 September 2024 ; Revised Form Accepted : 20 December 2024)

https://doi.org/10.56153/g19088-024-0218-67

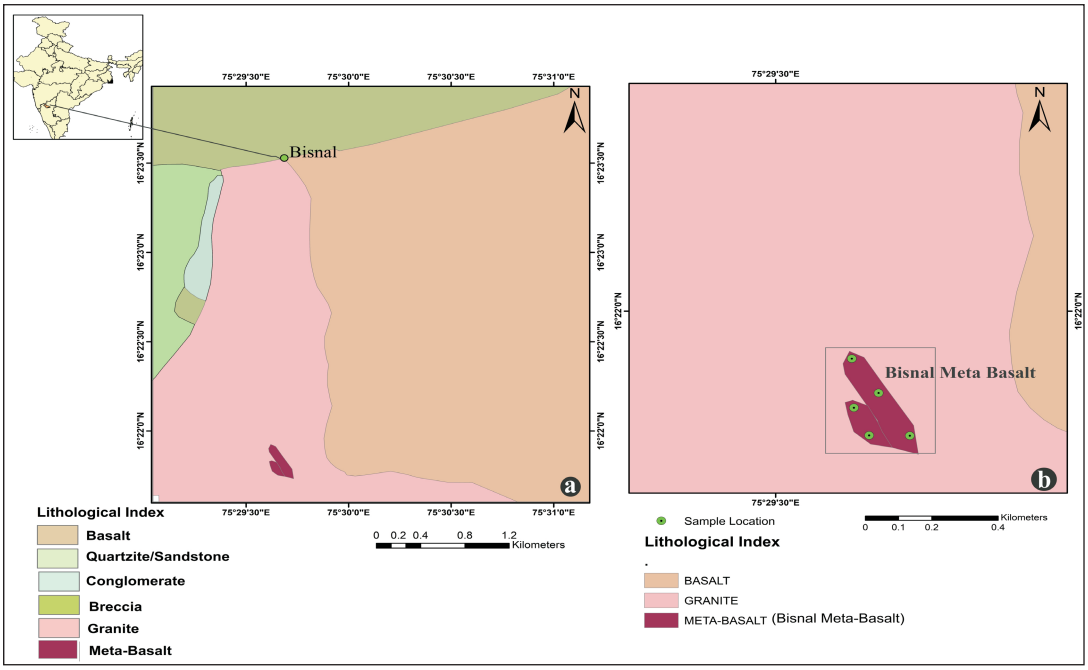

Fig.1. a) Lithological map of the area around Bisnal Taluk, Karnataka, b) Showing the sample location map.

geochemistry of metabasalts around Bisnal village to understand the elemental mobility and mantle crust contamination process coupled with tectonic aspects.

Geological Setting

The study area is located in the northwest region of the Bagalkot district at Bisnal village. Metabasalts are the characteristic feature that is seen in the south of Bisnal village. In the later course these metabasalts are intruded by the EDC younger granitoids which are of 2.5Ga. that is seen extending from Bilgi to Bisnal in the E-W direction, the enclaves of the metabasalts are seen in the granites that are exposed in the Bilgi town(Dey *et al.*, 2012), further the area is surrounded by the Kaladgi sediments belonging to the Bagalkot group which is evidenced by the quartzites, breccia and conglomerates of the Lokapur Subgroup. Over these sediments in the North and North Eastern directions the Deccan Basalts are present (Fig. 1).

Materials and Methods

The research was carried out including extensive fieldwork in the study area and the collection of representative rock samples. These rock samples were then subjected to detailed petrographic studies using a Leica Laborlux polarizing microscope available at DOS in Earth Science, University of Mysore, Mysore. The whole rock chemistry of the samples was carried out at the sample solution analytical lab in Wuhan, China. Major elements were analyzed on the fused glass beads using the Zsx Primus II wavelength dispersive X-ray fluorescence spectrometer (XRF) produced by RIGAKU, Japan. The test conditions are voltage: 50 kV, current: 60mA, and all major element analysis lines are kα, the standard curve uses the national standard material: rock standard sample GBW07101-14. Whole rock trace element analysis was carried out using Agilent 7700e ICP-MS, Chinese rock standards GSR-3 was used to compare the trace element concentrations obtained.

Petrography

The petrographic characteristics of these rocks show that they have undergone deformation, which is indicated by the presence of schistosity that is evidenced by the arrangement of alternate mafic and felsic minerals bands (Fig. 2a) that is made up of actinolite, hornblende, chlorite, epidote, plagioclase, muscovite, iron oxides such as magnetite, ilmenite, and sulphides like pyrite, chalcopyrite, and pyrrhotite. The occurrence of sulphides like pyrites and chalcopyrites indicate the primary magmatic as they occur in the disseminated form (Fig. 2e) along with also the hydrothermal origin is evidenced as they occur in the form of fracture filling in quartz carbonate veins (Fig. 2a-d). Based on the texture and mineral assemblage, lower green schist to epidote amphibolite facies metamorphism is seen in these rocks.

Whole Rock Geochemistry

Metabasalt rocks of the Bisnal village show consistency in the composition of major oxides. The whole rock chemistry data is given in Table 1. The major oxide composition are as follows SiO_2 (50.10-52.36%), TiO_2 (1.10-1.14%), Al_2O_3 (13.40-13.90%), Fe_2O_3 (11.89-14.66%), MgO (4.48-4.95%), CaO (8.52-9.20%), Na_2O (2.77-3.07%), MnO (0.18-0.20%), K_2O (0.72-0.77%), P_2O_5 (0.12-0.15%) and LOI (1.64-3.37%).

Results and Discussion

The major oxides data (%) show significant enrichment of TiO_2, Al_2O_3, Fe_2O_3, CaO, Na_2O, and LOI. The total alkali values are comparatively of low range *i.e.*, 3.49-3.85 %, with higher Na_2O than K_2O. The Co *vs* Th plot (Fig. 3a) shows the Calc alkaline trend for the rock samples (Hastie *et al.*, 2008). The Nb/Y vs Zr/TiO_2 plot (*after* Winchester and Floyd, 1977) (Fig. 3b) and Nb/Y *vs* Zr/Ti plot

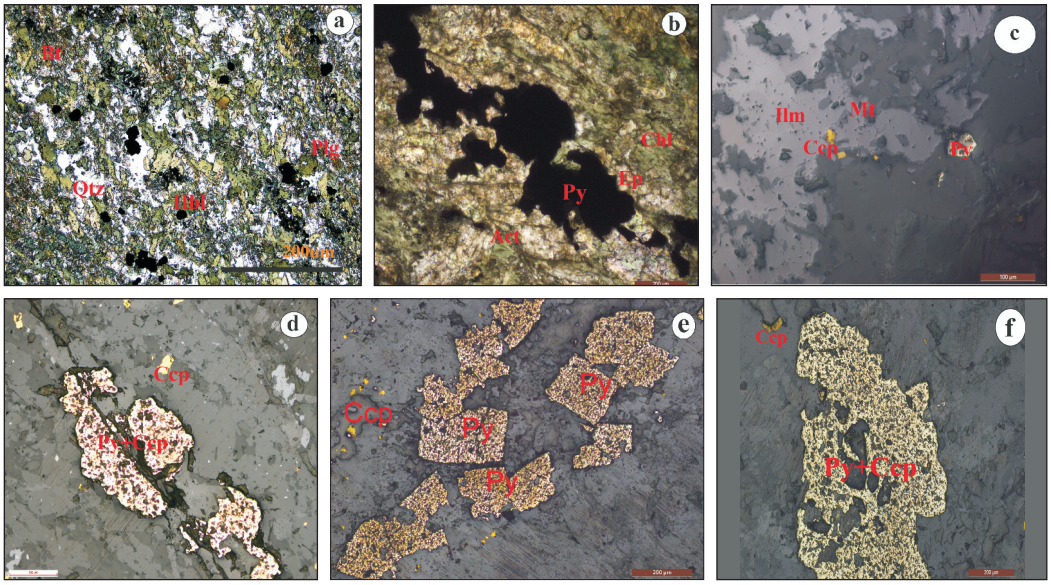

Fig 2. Photomicrograph of metabasalts a) Note the presence of silicate minerals such as Biotite, plagioclase, quartz and hornblende. b) Showing the presence of epidote, pyrites, chlorite and actinolite. c) showing the presence of ilmenite, magnetite, pyrite and chalcopyrite. d) observe the replacement of pyrite along the veins by chalcopyrit e) Showing the replacement of euhedral pyrite by chalcopyrite f) Scavenged pyrites by chalcopyrite.

(*after* Pearce, 1996; Fig.3c) shows the composition variation from basalts to andesite.

A plot of selected major oxides and the trace elements, mainly the HFSE, was plotted against MgO (MgO vs TiO_2, Fe_2O_3, Al_2O_3, P_2O_5, Nb, Zr, Ce, Y) to understand the rate of fractional crystallization process for a mafic melt (Fig. 4).

The TiO_2, Fe_2O_3, show a positive trend with MgO, but Al_2O_3, P_2O_5, Ce, Y and Zr show a negative trend with MgO, Nb ratios range from 3.77-4.23ppm which is comparatively and makes a vertical trend indicating low to moderate fractionation during the crystallisation process.

The trace elements analysis show a small enrichment in the LILE and moderate to flat patterns in the HFSE elements (Fig. 5a), with a strong depletion in the Nb is observed when the values are

Table 1: The whole rock chemistry data of metabasalts

Sample No.	Mb 01	Mb 02	Mb 03	Mb 04	Mb 05
SiO_2	51.06	50.11	52.37	50.16	50.14
TiO_2	1.10	1.13	1.12	1.14	1.12
Al_2O_3	13.91	13.40	13.84	13.46	13.43
Fe_2O_3	13.02	14.67	11.90	14.56	14.58
MnO	0.20	0.21	0.18	0.21	0.21
MgO	4.92	4.95	4.48	4.95	4.95
CaO	8.87	9.16	8.52	9.20	9.17
Na_2O	3.08	2.77	3.02	2.78	2.78
K_2O	0.78	0.72	0.74	0.72	0.72
P_2O_5	0.13	0.13	0.15	0.13	0.13
LOI	2.74	1.79	3.37	1.65	1.83
SUM	99.80	99.05	99.70	98.96	99.07
Li	16.6	17.6	17.7	17.1	17.9
Be	0.80	0.75	0.80	0.73	0.73
Sc	34.7	35.4	35.7	35.6	36.8
V	283	294	273	292	298
Cr	79.4	81.3	68.4	80.8	81.2
Co	38.5	48.2	31.5	48.0	53.3
Ni	57.2	61.1	47.3	58.7	64.0
Cu	153	166	149	166	178
Zn	106	115	94.1	113	120
Ga	18.5	18.3	17.7	17.9	18.4
Rb	31.1	25.4	28.3	25.1	25.5
Sr	239	216	259	216	220
Y	27.8	29.2	29.3	28.3	28.7
Zr	92.9	94.2	107	96.8	97.2
Nb	3.77	4.20	4.23	4.11	3.94
Sn	0.98	1.34	1.18	1.26	1.52
Cs	1.87	1.88	1.87	1.86	1.92
Ba	96.4	86.2	96.5	87.3	86.5

Sample No.	Mb 01	Mb 02	Mb 03	Mb 04	Mb 05
La	7.95	8.68	9.54	7.88	7.70
Ce	20.3	21.6	23.6	20.3	19.6
Pr	2.70	2.91	3.11	2.65	2.62
Nd	12.0	12.5	13.5	12.1	11.7
Sm	3.45	3.75	3.77	3.61	3.42
Eu	1.14	1.19	1.23	1.18	1.17
Gd	4.14	4.37	4.40	4.13	4.18
Tb	0.74	0.78	0.77	0.72	0.74
Dy	4.89	5.17	5.19	4.94	4.93
Ho	1.02	1.09	1.09	1.03	1.05
Er	2.95	3.09	3.18	3.00	3.01
Tm	0.44	0.47	0.47	0.44	0.46
Yb	3.01	3.19	3.04	3.13	3.13
Lu	0.45	0.48	0.47	0.46	0.46
Hf	2.54	2.65	2.90	2.70	2.70
Ta	0.26	0.30	0.29	0.27	0.27
Tl	0.17	0.16	0.16	0.16	0.16
Pb	4.94	6.71	5.41	6.93	6.80
Th	1.40	1.64	1.94	1.31	1.39
U	0.47	0.48	0.61	0.42	0.45
(La/Sm)N	1.44	1.45	1.59	1.37	1.41
Sum REE	65.18	69.27	73.36	65.57	64.17
$(Gd/Yb)_N$	1.13	1.13	1.17	1.09	1.10
La/Yb	2.64	2.72	3.14	2.51	2.46
Dy/Yb	1.62	1.62	1.71	1.57	1.57
Ce/Ce*	1.05	0.87	0.88	1.06	1.04
Th/LA	0.18	0.19	0.20	0.17	0.18
Nb/Y	0.14	0.14	0.14	0.15	0.14
Zr/Hf	36.61	35.58	37.01	35.85	36.04
Y/Ho	27.40	26.88	26.77	27.54	27.38

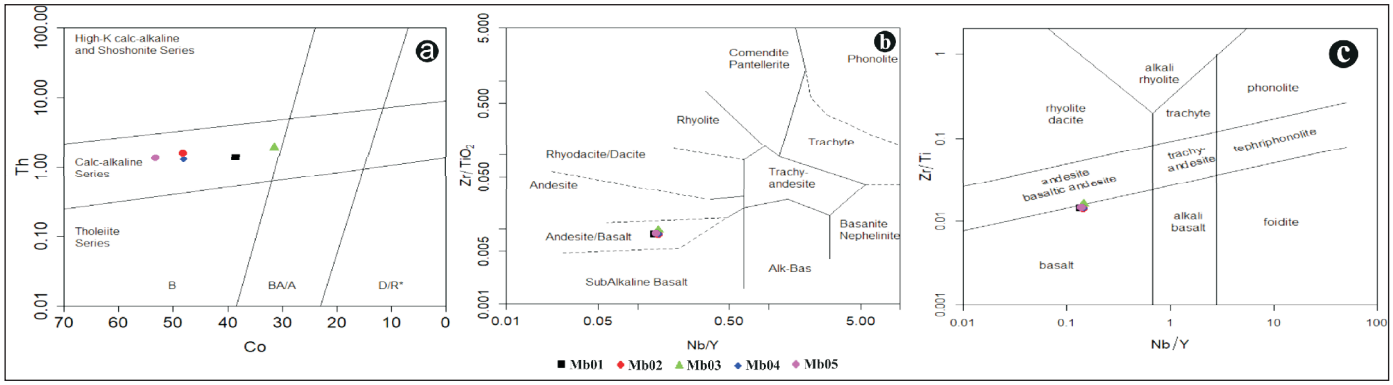

Fig.3. a) Co-Th Plot after Hastie *et al.* (2008) for basalts; the calc-alkaline magma series trend is seen for the metabasalts, b) Nb/Y *vs* Zr/TiO_2 classification plot for basalts after Winchester and Floyd (1977), c) Plot of Nb/Y *vs* Zr/Ti for basalts (*After* Pearce, 1996).

correlated with that of the primitive mantle values in the plot (*after* Sun and McDonough, 1989).

The chondrite normalized REE plot (*after* Anders and Grevesse, 1989) show a minute enriched to flat LREE and an almost flat HREE pattern (Fig 5b). The $[(La)_N/(Yb)_N]$ LREE/HREE ratio is 1.70-2.17 for all the samples, which indicates a slight enrichment of LREE elements.

The HREE $(Gd)_N/(Yb)_N$ ratio is 1.09-1.13, which shows a very minor depletion compared to that of the LREE elements. The Eu/Eu* ratio is slightly negative for all the samples, varying between 0.89 and 0.93. From this, we can infer that the plagioclase fractionation was very low.

Elemental Mobility and Alteration

As these metabasalts belong to the NW extension of the HK Schist belt (Dey *et al.,* 2015), it is necessary to understand the geochemical signature of these samples with respect to Archean mafic volcanism. The common alteration feature that the Archean metabasalts show is hydrothermal alteration and the change in the grade of metamorphism *i.e.* from greenschist to amphibolite facies (Chandan Kumar and Ugarkar, 2017; Said *et al.*, 2010). The metabasalt of the study area clearly indicate the hydrothermal alteration by the presence of the sulphide minerals such as pyrite and chalcopyrite and the occurrence of the silicate minerals such as actinolite, hornblende, chlorite, plagioclase, biotite, and epidote which indicates that there is a increase in the metamorphic grade from the upper greenschist to epidote amphibolite facies. This is also supported by the ratios of CHARAC twin pairs of Y/Ho (26.77-27.54ppm) and Zr/Hf (35.58-37.01ppm) indicates that these rocks have been modified under the aqueous systems (Bau and Bau, 1996). LOI values of the metabasalts are a good indicator of the mineral alterations (Polat, 2012). For the analysed rock suites, the LOI values range from (1.6%-3.3%). Along with that, the major elements Na, K and Ca show slight deviation from their normal values, indicating the elemental mobility in the metabasalts. It can be evidenced from the previous works that the elements such as the HFSE elements such as Nb, Th, Zr, Hf and Ta are not very mobile

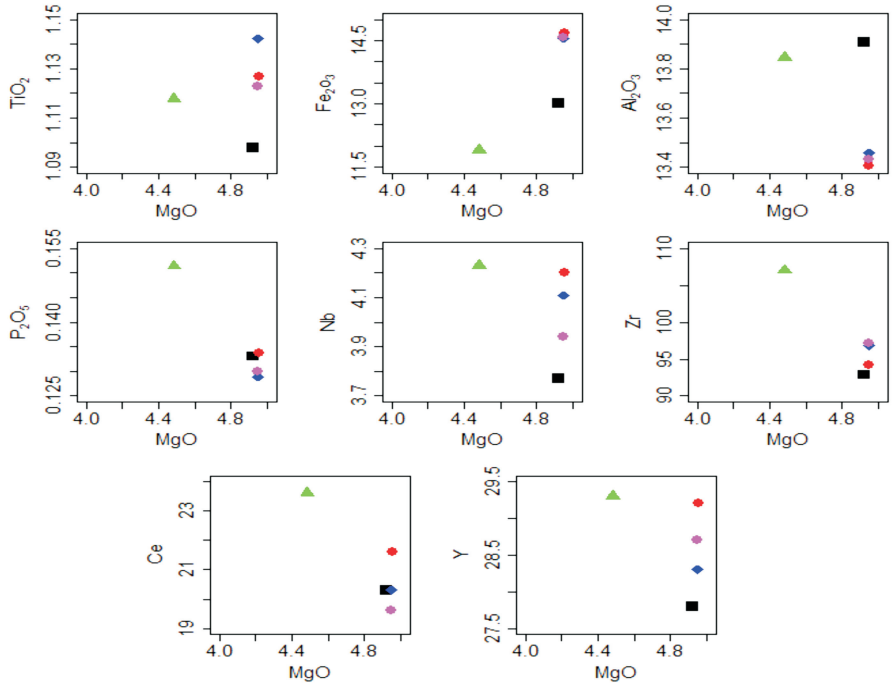

Fig.4. The Harker's plot of MgO *vs* Selected major and trace elements (MgO *vs* MgO *vs* TiO_2, Fe_2O_3, Al_2O_3, P_2O_5, Nb, Zr, Ce, Y.)

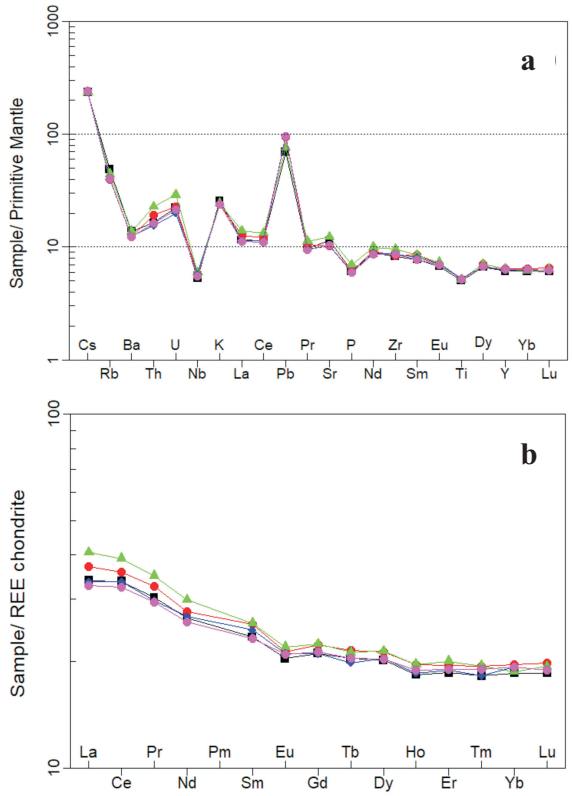

Fig.5. a) The multielement plot for metabasalts (*After* Sun and McDonough, 1989), b) the REE plot of Metabasalts (*After* Anders and Grevesse, 1989).

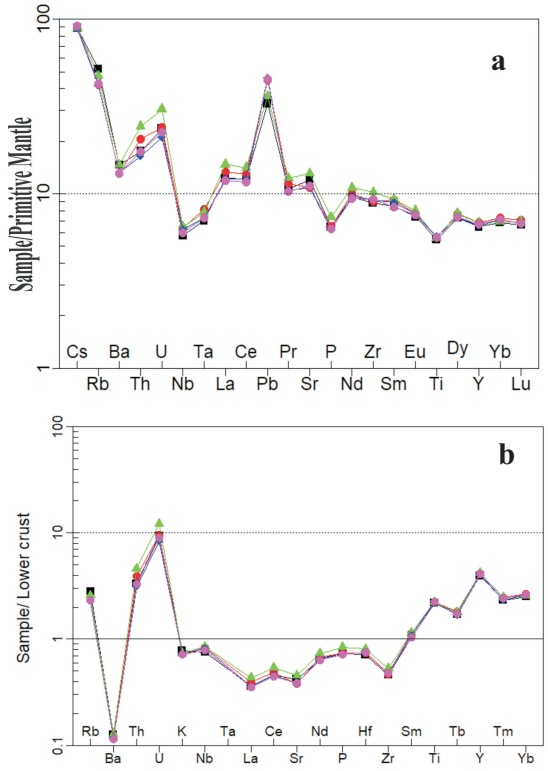

Fig. 6. a) Trace element vs normalised primitive value diagram (*After* Sun and McDonough, 1995), b) lower crust *vs* Trace element diagram (*After* Weaver and Tarney, 1984).

(Arndt, 1994; Humphris and Thompson, 1978; Jochum *et al.*, 1991; Manikyamba *et al.*, 2009, 2014, 2015 and references therein; Said *et al.*, 2010) but in the current studied suite of rocks it can be noticed that there is a minor variation in these elements of metabasalts, which indicates the elemental mobility and the magma crust interaction process. The Ce/Ce* anomaly range for the archean volcanic sequence should be between 0.9 to 1.1(Manikyamba *et al.*, 2015; Polat, 2012). However, for the current suite of rock samples, the Ce/Ce* anomaly values range is <0.9 for two samples (Mb02, Mb03), which shows that there is mobility of LREE elements such as La, Ce, Pr, Nd, Sm whereas for the remaining samples, the Ce/Ce* is within 0.9-1.1, indicating low elemental mobility.

Crustal Contamination

The interaction with the crust modifies the chemical compositions in the magma (Singh *et al.,* 2020). The petrography of the current suite of metabasaltic rocks shows the mineral assemblage, which indicates the change in the metamorphic grade from upper greenschist to epidote amphibolite facies along with the presence of sulphide mineralization, which is attributed to both primary magmatic and secondary hydrothermal origin. This indicates the contamination of the magma. The lesser abundance of the Ni values (47.30-64.0 ppm), lesser Cr values (68.40-81.30 ppm), and the lower range of MgO (4.48-4.95%) suggest that the magma is not of original composition and it has been significantly contaminated during the crystallization process. Ratios of Th/La (0.17-0.20) are higher than that of the primitive mantle (0.12) given by Sun and McDonough (1995) (Fig. 6a). Similarly, the ratios of Nb/Y (0.14-0.15) are also very much higher than that of the lower crust values (0.7) as given by Weaver and Tarney (1984) (Fig. 6b) and shows clear change in the geochemistry of metabasalts.

Conclusions

The calc-alkaline composition of metabasalts around Bisnal village forms the northwest extension of the H-K schist belt. These rocks indicate the elemental mobility effects due to hydrothermal alteration and by the change in the grade of metamorphism. The ratios of Th/La and Nb/Y indicate that these metabasalts show a higher degree of crustal contamination.

Authors' Contributions

TBM: Field Work and Sample Collection, Analysis, Conceptualization and Manuscript Preparation. **MP**: Visualization and Editing. **PNKN**: Supervision and Editing. **SKBV**: Fieldwork, Supervision and Reviewing.

Conflict of Interest

Authors declare no conflict of interest.

Acknowledgements

The authors express their sincere gratitude to the Chairman, DOS in Earth Sciences, University of Mysore, Manasagangotri, for the constant encouragement during the studies. The authors also thank the editor and anonymous reviewers of the JGSR journal for their help in improving the quality of this paper.

References

Anders, E. and Grevesse, N. (1989). Abundances of the elements: Meteoritic and solar. Geochim. Cosmochim. Act., v. 53(1), pp. 197-214.

Arndt, N.T. (1994). Archean komatiites. In: Developments in Precambrian Geology, Elsevier, v. 11, pp. 11–44.

Bau, M. and Bau, M. (1996). Controls on the fractionation of isovalent trace elements in magmatic and aqueous systems: evidence from Y/Ho, Zr/Hf, and lanthanide tetrad effect. *In*: Contrib. Mineral. Petrol., Springer-Verlag, v. 123.

Bennett, V.C. (2003). Compositional evolution of the mantle. Treat. Geochem., v. 2, 568p.

Chandan-Kumar, B. and Ugarkar, A.G. (2017). Geochemistry of mafic–ultramafic magmatism in the Western Ghats belt (Kudremukh greenstone belt), western Dharwar Craton, India: implications for mantle sources and geodynamic setting. Int. Geol. Rev., v. 59, pp. 1507-1531.

Condie, K.C. and Aster, R.C. (2013). Refinement of the supercontinent cycle with Hf, Nd and Sr isotopes. Geosci. Front., v. 4(6), pp. 667–680.

Condie, K.C. and Kröner, A. (2013). The building blocks of continental crust: evidence for a major change in the tectonic setting of continental growth at the end of the Archean. Gond. Res., v. 23(2), pp.394–402.

Dey, S., Pandey, U.K., Rai, A.K. and Chaki, A. (2012). Geochemical and Nd isotope constraints on petrogenesis of granitoids from NW part of the eastern Dharwar craton: Possible implications for late Archaean crustal accretion. Jour. Asian Earth Sci., v. 45, pp.40–56.

Hastie, A.R., Kerr, A.C., Mitchell, S.F. and Millar, I.L. (2008). Geochemistry and petrogenesis of Cretaceous oceanic plateau lavas in eastern Jamaica. Lithos, v. 101(3), pp. 323–343. https://doi.org/https://doi.org/10.1016/j.lithos.2007.08.003

Humphris, S.E. and Thompson, G. (1978). Trace element mobility during hydrothermal alteration of oceanic basalts. Geochim. Cosmochim. Act., v. 42(1), pp.127–136.

Jochum, K.P., Arndt, N.T. and Hofmann, A.W. (1991). Nb-Th-La in komatiites and basalts: constraints on komatiite petrogenesis and mantle evolution. Earth Planet. Sci. Lett., v. 107(2), pp. 272–289.

Kerrich, R. and Xie, Q. (2002). Compositional recycling structure of an Archean super-plume: Nb–Th–U–LREE systematics of Archean komatiites and basalts revisited. Contrib. Mineral. Petrol., v. 142(4), pp. 476–484.

Lafleche, M.R., Dupuy, C. and Dostal, J. (1992). Tholeiitic volcanic rocks of the late Archean Blake River Group, southern Abitibi greenstone belt: origin and geodynamic implications. Canad. Jour. Earth Sci., v. 29(7), pp. 1448–1458.

Ludden, J., Gélinas, L. and Trudel, P. (1982). Archean metavolcanics from the Rouyn–Noranda district, Abitibi Greenstone Belt, Quebec. 2. Mobility of trace elements and petrogenetic constraints. Canad. Jour. Earth Sci., v. 19(12), pp. 2276–2287.

MacLean, W.H. and Kranidiotis, P. (1987). Immobile elements as monitors of mass transfer in hydrothermal alteration; Phelps Dodge massive sulfide deposit, Matagami, Quebec. Econ. Geol., v. 82(4), pp. 951-962.

Mahantesha, P., Prakash Narasimha, K., Shareef, M., Gopala Krishna, G. and Rahim, T. (2021). Cobalt Mineralization Associated With Copper from Kalyadi Area, Western Dharwar Craton, South India. Jour. Geosci. Res., v. 6 (2), 136-145.

Manikyamba, C., Ganguly, S. and Pahari, A. (2021). Geochemical Features of Bellara Trap Volcanic Rocks of Chitradurga Greenstone Belt, Western Dharwar Craton, India: Insights into MORB-BABB Association from a Neoarchean Back-Arc Basin. Jour. Earth Sci., v. 32(6), pp.1528–1544.

Manikyamba, C., Ganguly, S., Saha, A., Santosh, M., Singh, M.R. and Rao, D.V.S. (2014). Continental lithospheric evolution: constraints from the geochemistry of felsic volcanic rocks in the Dharwar Craton, India. Jour. Asian Earth Sci., v. 95, pp. 65–80.

Manikyamba, C., Ganguly, S., Santosh, M., Singh, M. R., and Saha, A. (2015). Arc-nascent back arc signature in metabasalts from the Neoarchaean Jonnagiri greenstone terrane, Eastern Dharwar Craton, India. Geol. Jour., v. 50(5), pp. 651–669.

Manikyamba, C., Kerrich, R., Khanna, T.C., Satyanarayanan, M. and Krishna, A.K. (2009). Enriched and depleted arc basalts, with Mg-andesites and adakites: a potential paired arc–back-arc of the 2.6 Ga Hutti greenstone terrane, India. Geochim. Cosmochim. Act., v. 73(6), pp.1711–1736.

McDonough, W.F. and Sun, S.S. (1995). The composition of the Earth. Chem. Geol., v. 120(3), pp. 223–253. https://doi.org/https://doi.org/10.1016/0009-2541(94)00140-4

Naqvi, S.M., Khan, R.M.K., Manikyamba, C., Mohan, M.R. and Khanna, T.C. (2006). Geochemistry of the NeoArchaeanhigh-Mg basalts, boninites and adakites from the Kushtagi–Hungund greenstone belt of the Eastern Dharwar Craton (EDC); implications for the tectonic setting. Jour. Asian Earth Sci., v. 27(1), pp. 25–44.

Pahari, A., Tang, L., Manikyamba, C., Santosh, M., Subramanyam, K.S.V. and Ganguly, S. (2019). Meso-Neoarchean magmatism and episodic crustal growth in the Kudremukh-Agumbe granite-greenstone belt, western Dharwar Craton, India. Precamb. Res., v. 323, pp. 16–54.

Patra, K., Anand, R., Balakrishnan, S. and Dash, J.K. (2020). Geochemistry of ultramafic–mafic rocks of Mesoarchean Sargur Group, western Dharwar craton, India: Implications for their petrogenesis and tectonic setting. Jour. Earth Syst. Sci., v. 129, pp.1–29.

Pearce, J.A. (2014). Geochemical fingerprinting of the Earth's oldest rocks. Geology, v. 42(2), pp.175–176.

Polat, A. (2012). Growth of Archean continental crust in oceanic island arcs. Geology, v. 40(4), pp. 383.

Said, N., Kerrich, R. and Groves, D. (2010). Geochemical systematics of basalts of the Lower Basalt Unit, 2.7 Ga Kambalda Sequence, Yilgarn craton, Australia: plume impingement at a rifted craton margin. Lithos, v. 115(1-4), pp.82-100.

Singh, M.R., Singh, A.K., Santosh, M., Lingadevaru, M. and Lakhan, N. (2020). Neoarchean arc□back arc subduction system in the Indian Peninsula: Evidence from mafic magmatism in the Shimoga greenstone belt, western Dharwar Craton. Geol. Jour., v. 55(7), pp. 5308-5329.

Sun, S.S. and McDonough, W.F. (1989). Chemical and isotopic systematics of oceanic basalts: implications for mantle composition and processes. Geol. Soc., London, Spec. Publ., v. 42(1), pp. 313-345.

Taylor, S.R. and McLennan, S.M. (1995). The geochemical evolution of the continental crust. Rev. Geophys., v. 33(2), pp. 241-265.

Weaver, B.L. and Tarney, J. (1981). Chemical changes during dyke metamorphism in high-grade basement terrains. Nature, v. 289(5793), pp.47-49.

Weaver, B.L. and Tarney, J. (1984). Empirical approach to estimating the composition of the continental crust. Nature, v. 310(5978), pp. 575-577.

Winchester, J.A. and Floyd, P.A. (1977). Geochemical discrimination of different magma series and their differentiation products using immobile elements. Chem. Geol., v. 20, pp. 325-343.